

AD-A121 796

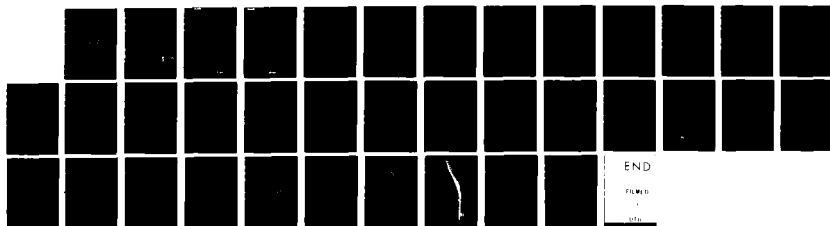
COMPUTATION OF DISCRETE SLANTED HOLE FILM COOLING FLOW  
USING THE NAVIER-S. (U) SCIENTIFIC RESEARCH ASSOCIATES  
INC GLASTONBURY CT H J GIBELING ET AL. JUL 82  
R82-910002-4 AFOSR-TR-82-1004

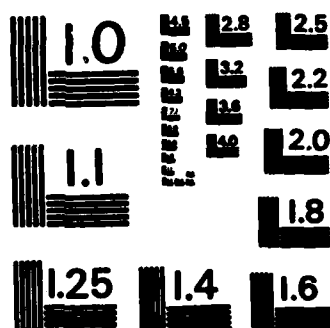
1/1

UNCLASSIFIED

F/G 13/1

NL





MICROCOPY RESOLUTION TEST CHART  
NATIONAL BUREAU OF STANDARDS-1963-A

AFOSR-TR- 82 - 1004

Report R82-910002-4 ✓

AD A121796

COMPUTATION OF DISCRETE SLANTED HOLE FILM COOLING FLOW  
USING THE NAVIER-STOKES EQUATIONS

H. J. Gibeling, S. J. Shamroth and H. McDonald  
Scientific Research Associates, Inc.  
P.O. Box 498  
Glastonbury, CT 06033

July 1982

Prepared for:

Air Force Office of Scientific Research

DTIC  
ELECTE  
NOV 23 1982  
S D  
E

Approved for public release;  
distribution unlimited.

THIS FILE COPY

**UNCLASSIFIED**

SECURITY CLASSIFICATION OF THIS PAGE (When Data Entered)

AGE (When Data Entered)

REPORT DOCUMENTATION PAGE		READ INSTRUCTIONS BEFORE COMPLETING FORM
1. REPORT NUMBER <b>AFOSR-TR- 82-1004</b>	2. GOVT ACCESSION NO. <b>AD-A121796</b>	3. RECIPIENT'S CATALOG NUMBER
4. TITLE (and Subtitle) <b>Computation of Discrete Slanted Hole Film Cooling Flow Using the Navier-Stokes Equations</b>		5. TYPE OF REPORT & PERIOD COVERED <b>Annual Technical Report 81 April 1 to 82 March 31</b>
		6. PERFORMING ORG. REPORT NUMBER
7. AUTHOR(s) <b>H. J. Gibeling, S. J. Shamroth and H. McDonald</b>		8. CONTRACT OR GRANT NUMBER(s) <b>F49620-78-C-0038</b>
9. PERFORMING ORGANIZATION NAME AND ADDRESS <b>Scientific Research Associates, Inc. P.O. Box 498 Glastonbury, CT 06033</b>		10. PROGRAM ELEMENT, PROJECT, TASK AREA & WORK UNIT NUMBERS <b>61102F 2307/A4</b>
11. CONTROLLING OFFICE NAME AND ADDRESS <b>Air Force Office of Scientific Research /NA Building 410, Bolling AFB, DC 20332</b>		12. REPORT DATE <b>July 1982</b>
14. MONITORING AGENCY NAME & ADDRESS (if different from Controlling Office)		13. NUMBER OF PAGES <b>35</b>
		15. SECURITY CLASS. (of this report) <b>Unclassified</b>
		15a. DECLASSIFICATION/DOWNGRADING SCHEDULE
16. DISTRIBUTION STATEMENT (of this Report)  <b>Approved for public release; distribution unlimited.</b>		
17. DISTRIBUTION STATEMENT (of the abstract entered in Block 20, if different from Report)  <b>Approved for public release; distribution unlimited.</b>		
18. SUPPLEMENTARY NOTES		
19. KEY WORDS (Continue on reverse side if necessary and identify by block number)  <b>Film Cooling Navier-Stokes Equations Zone Embedding Interactive Boundary Conditions</b>		
20. ABSTRACT (Continue on reverse side if necessary and identify by block number) <b>An analysis and computational procedure have been developed for predicting flow and heat transfer which results from coolant injection through a single row of round holes oriented at an angle to a flat surface with the injection and free stream velocity vectors coplanar. This method solves the compressible Navier-Stokes equations and utilizes "zone embedding", surface-oriented coordinates, interactive boundary conditions, and an efficient split LBI scheme. The approach treats the near-hole flow region where the film cooling flow is initially established. Prior studies considered only laminar flow in order to simplify</b>		

DD FORM 1473

1 JAN 73

EDITION OF 1 NOV 65 IS OBSOLETE

**UNCLASSIFIED**


SECURITY CLASSIFICATION OF THIS PAGE (When Data Entered)

**UNCLASSIFIED**

SECURITY CLASSIFICATION OF THIS PAGE

(When Data Entered)

development of the computational procedure. Under the present effort, several turbulence models suitable for the discrete hole film cooling problem have been investigated by predicting a number of test cases from the 1980-81 AFOSR-HTTM-Stanford Conference on Complex Turbulent Flows. The calculation of a discrete hole film cooling case for an injection angle of 35 degrees has been initiated using a mixing length turbulence model. These results will be compared with the experimental data of Kadotani and Goldstein, a recalculation with either a turbulence kinetic energy/algebraic length scale or a turbulence kinetic energy/dissipation rate model would be carried out under the subsequent effort, if warranted by the data comparison.



**UNCLASSIFIED**

SECURITY CLASSIFICATION OF THIS PAGE (When Data Entered)

# TABLE OF CONTENTS

	Page
ABSTRACT . . . . .	1
INTRODUCTION . . . . .	2
PREVIOUS WORK . . . . .	4
TURBULENCE MODELS . . . . .	7
RESULTS . . . . .	11
Stanford Case 0423 . . . . .	11
Stanford Case 8601 . . . . .	12
Stanford Case 8641 . . . . .	14
Turbulent Film Cooling Flow . . . . .	15
REFERENCES . . . . .	16
FIGURES . . . . .	18

Accession For	
NTIS GRA&I	<input checked="" type="checkbox"/>
DTIC TAB	<input type="checkbox"/>
Unannounced	<input type="checkbox"/>
Justification	
By	
Distribution/	
Availability Codes	
Dist	Avail and/or Special
A	



AIR FORCE OFFICE OF SCIENTIFIC RESEARCH (AFSC)  
 NOTICE OF REPLYING TO DTIC  
 This technical report has been reviewed and is  
 approved for release under AFM 193-12.  
 Distribution is unlimited.  
 MATTHEW J. NEMER  
 Chief, Technical Information Division

Computation of Discrete Slanted Hole Film  
Cooling Flow Using the Navier-Stokes Equations

by

H. J. Gibelung, S. J. Shamroth and H. McDonald  
Scientific Research Associates, Inc.  
P.O. Box 498  
Glastonbury, CT 06033

ABSTRACT

An analysis and computational procedure have been developed for predicting flow and heat transfer which results from coolant injection through a single row of round holes oriented at an angle to a flat surface with the injection and free stream velocity vectors coplanar. This method solves the compressible Navier-Stokes equations and utilizes "zone embedding", surface-oriented coordinates, interactive boundary conditions, and an efficient split LBI scheme. The approach treats the near-hole flow region where the film cooling flow is initially established. Prior studies considered only laminar flow in order to simplify development of the computational procedure. Under the present effort, several turbulence models suitable for the discrete hole film cooling problem have been investigated by predicting a number of test cases from the 1980-81 AFOSR-HTTM-Stanford Conference on Complex Turbulent Flows. The calculation of a discrete hole film cooling case for an injection angle of 35 degrees has been initiated using a mixing length turbulence model. These results will be compared with the experimental data of Kadotani and Goldstein, and recalculation with either a turbulence kinetic energy/algebraic length scale or a turbulence kinetic energy/dissipation rate model would be carried out under the subsequent effort, if warranted by the data comparison.

## INTRODUCTION

To achieve higher turbine efficiencies, designers have been forced to deal with high turbine inlet temperatures which may exceed structural limitations of available materials used for turbine blades unless some method of cooling these blades is introduced. Various cooling schemes have been devised to ensure that the structural integrity of the blades remain intact when exposed to a high temperature environment for prolonged periods of time. One of the more promising schemes is discrete hole film cooling, wherein cooling air is injected through either a single row or multiple staggered rows of holes, to provide a protective layer of cool air between the blade surface and hot mainstream gases. Discrete hole film cooling is better suited to the high temperatures of advanced high performance engines than the current convectively cooled blades found in commercial engines. A large number of parameters can be varied to obtain a configuration which optimizes heat transfer and aerodynamic characteristics, including hole shapes and patterns, injection angles and rates, surface curvature, coolant temperatures, and mainstream boundary layer characteristics. Since experimental determination of optimal configurations is costly, a computational procedure which could be used to screen alternative configurations without experimental testing would be of considerable value. An analysis and computational procedure were developed previously for predicting flow and heat transfer which results from coolant injection through a single row of round holes oriented at a non-normal angle to a flat surface. This work was an extension of a previous effort which considered only normal injection through a single row of round holes. Both of these prior studies considered only laminar flow in order to simplify development of the computational procedure. The present effort involves investigation of turbulence models suitable for the discrete hole film cooling problem. Therefore, the model chosen must be capable of treating flows with large pressure gradients and separated regions. Several turbulence models were investigated under the present study by predicting a number of test cases from the 1980-81 AFOSR-HTTM-Stanford Conference on Complex Turbulent Flows.\* The models considered were:

---

\*Two of the cases reported on herein were partially funded by AFOSR and the U.S. Army Research Office.



(1) algebraic mixing length ( $\ell$ ), (2) turbulence kinetic energy and algebraic length scale ( $k-\ell$ ), and (3) turbulence kinetic energy and dissipation rate ( $k-\epsilon$ ). All of these models utilize an isotropic eddy viscosity formulation to represent the Reynolds stress terms. This study will ultimately provide an improved understanding of the turbulent flow film cooling process, particularly in the near-hole region, and represents the third step toward development of a computer program capable of predicting heat transfer and aerodynamic loss levels associated with discrete hole film cooling on gas turbine blades.

## PREVIOUS WORK

Previous experimental work on film cooling flow has consisted mainly of flow visualization studies and measurements of film cooling effectiveness downstream of the coolant injection hole for a variety of flow conditions. For example, Colladay and Russell [1] performed a flow visualization study of discrete hole film cooling in three different hole configurations, to obtain a better understanding of flow behavior associated with coolant injection. They considered injection from discrete holes in a three-row staggered array with five-diameter spacing and three-hole angles: (1) normal to the surface, (2) slanted 30 degrees to the surface but aligned (coplanar) with the free stream, and (3) slanted 30 degrees to the surface and 45 degrees laterally to the free stream. For flow conditions typical of gas turbine applications, Colladay and Russell observed that normal injection is subject to flow separation even at low injection rates, that slanted injection works well except at high injection rates, and that compound slanted-yawed injection is less susceptible to separation but tends to promote entrainment of free stream fluid (which augments heat transfer) and to increase secondary flow losses. These experimental observations emphasize the importance of interaction between the injected fluid and the free stream.

Kadotani and Goldstein [2] have performed experimental measurements for discrete hole film cooling through a row of holes having three-diameter lateral spacing, inclined at 35 degrees to the injection surface, and coplanar with the free stream. They considered a variety of flow conditions and varied boundary layer thickness and injection rates, as well as Reynolds number and turbulence properties. They measured lateral and streamwise distributions of film cooling effectiveness downstream of injection, and also measured mean velocity and temperature in a transverse plane normal to the free stream and located at the downstream edge of the injection holes. Kadotani and Goldstein deduced from their measurements that reversed flow is present near the injection hole even for injection rates as low as 0.35, and that the size and strength of the reversed flow increases with increasing boundary layer thickness. They also found that the approaching boundary layer thickness significantly affects the flow behavior and lateral variation of film cooling effectiveness, particularly near the injection hole.

In a prior study of injection through a single array of round holes oriented normal to a flat surface, Kreskovsky, Briley and McDonald [3] solved the compressible Navier-Stokes equations utilizing surface-oriented coordinates and an efficient, consistently-split LBI scheme. Subsequently, Gibeling, Kreskovsky, Briley and McDonald [4] extended the work of [3] to treat the coolant injection through a single row of round holes oriented at a non-normal angle to a flat surface. In this analysis the governing equations in Cartesian coordinates were cast into strong conservation form using a Jacobian transformation to obtain the governing equations in a general nonorthogonal coordinate system. Both previous studies [3 and 4] focused on the near-hole flow region where the film cooling flow is initially established and where local hot spots may occur. Since the flow field surrounding injection may involve separation and reversed flow relative to the free stream, and since directional and/or other properties of the flow which might permit simplifying assumptions are not clearly evident, these analyses are based on numerical solution of the three-dimensional compressible Navier-Stokes equations. In selecting the computational domain, a "zone embedding" approach is adopted by [3,4] whereby attention is focused on a subregion of the overall flow field in the immediate vicinity of the discrete hole coolant injection. At the curved boundaries located within the free stream region, interactive boundary conditions which permit inflow and outflow of shear layers and the compressible inviscid free stream are derived from an assumed flow structure. Since details of the coolant velocity distribution at the hole exit are not known a priori and presumably will depend on an interaction between the coolant and the free stream flow, the computational domain is chosen to include the flow region within the coolant hole as well as that exterior to the hole. Including the flow region within the coolant hole permits the interaction between the coolant and free stream flows and its important influence near the hole to be determined as part of the final solution, without the need for simplifying assumptions. Sample laminar calculations yielded predictions of the interaction between the injectant and main stream flow which were in qualitative agreement with experimental observations.

The only other previous computational study known to the authors which treated the discrete hole film cooling problem using a three-dimensional calculation procedure is that of Bergeles, Gosman and Launder [5], who applied the approximate "partially parabolic" calculation procedure of Prataap & Spalding [6] for the case of laminar flow. This calculation procedure neglects

streamwise diffusion and employs iterated forward marching solution of three approximate momentum equations. The procedure begins with a "guessed" pressure field and performs iterated forward marching sweeps of the three-dimensional flow field, solving the approximate momentum equations and utilizing various strategies to modify or correct the pressure field, so as to improve the continuity balance. Since the calculation procedure is based on forward marching, the flow region within the coolant injection hole is excluded from the computational domain, and instead, the coolant velocity distribution is specified at the hole exit as a two-dimensional uniform stream at a prescribed injection angle. Bergeles, Gosman and Launder made flow calculations for several flow conditions, including different injection angles.

## TURBULENCE MODELS

This section presents the turbulence model equations in the general form utilized in the test cases considered herein. Details concerning algebraic length scale specification are given in the sections describing each test case, since the length scale formulation must be adapted to the particular flow being computed. The latter requirement is a major disadvantage of models using a specified length scale; therefore, consideration is given to the two-equation (k-ε) model [7,8] with appropriate low turbulence Reynolds number corrections [8] to permit sublayer resolution.

### Turbulence Kinetic Energy Equation

Several cases presented in this report utilize a turbulence kinetic energy equation and an algebraic length scale equation. The turbulence kinetic equation as given by [7,8] is

$$\frac{\partial(\rho k)}{\partial t} + \nabla \cdot (\rho \bar{u} k) = \nabla \cdot \left[ \left( \mu + \frac{\mu_T}{\sigma_k} \right) \nabla k \right] + \mu_T (2 \bar{D} : \bar{D}) - \rho \epsilon - 2 \mu (\nabla k^{1/2}) \cdot (\nabla k^{1/2}) \quad (1)$$

where k is the turbulence kinetic energy,

$$k = \frac{1}{2} \overline{\bar{u}^i \cdot \bar{u}^i} \quad (2)$$

### Turbulence Energy Dissipation Equation

The equation for the dissipation rate of turbulence energy, ε, as given by [7,8] is

$$\begin{aligned} \frac{\partial(\rho \epsilon)}{\partial t} + \nabla \cdot (\rho \bar{u} \epsilon) = & \nabla \cdot \left[ \left( \mu + \frac{\mu_T}{\sigma_\epsilon} \right) \nabla \epsilon \right] + C_1 \frac{\epsilon}{k} \mu_T (2 \bar{D} : \bar{D}) - C_2 \frac{\rho \epsilon^2}{k} \\ & - 2 \frac{\mu \mu_T}{\rho} \sum_{j,l=1}^3 \left( \frac{\partial^2 \bar{u}}{\partial x_j \partial x_l} \right) \cdot \left( \frac{\partial^2 \bar{u}}{\partial x_j \partial x_l} \right) \end{aligned} \quad (3)$$

where the deformation tensor  $\bar{D}$  is

$$\bar{D} = \frac{1}{2} [(\nabla \bar{u}) + (\nabla \bar{u})^T] \quad (4)$$

The turbulent flow stress tensor (Reynolds stress) which appears in the momentum conservation equations [9,10] is modeled using an isotropic eddy viscosity formulation, i.e.,

$$\pi^T = -\rho \overline{u^i u^j} = 2\mu_T \bar{D} - \frac{2}{3} \mu_T \nabla \cdot \bar{u} \quad (5)$$

The turbulent viscosity  $\mu_t$  appearing in Eqs. (1,3,5) must be determined using a suitable model, and the parameters  $\sigma_k$ ,  $\sigma_\epsilon$ ,  $C_1$  and  $C_2$  must be specified.

#### Turbulence Model Relations

The turbulent viscosity introduced above is obtained from the Prandtl-Kolmogorov relation viz.

$$\mu_T = C_\mu \frac{\rho k^2}{\epsilon} \quad (6)$$

When the dissipation rate equation (3) is not solved,  $\epsilon$  is determined from

$$\epsilon = C_\mu^{3/4} \frac{k^{3/2}}{l} \quad (7)$$

where the turbulence length scale,  $l$ , must be specified consistent with the expected turbulence structure of the flow.

The constraints  $\sigma_k$ ,  $\sigma_\epsilon$  and  $C_1$  are taken as [7],

$$\begin{aligned} \sigma_k &= 1.0 \\ \sigma_\epsilon &= 1.3 \\ C_1 &= 1.44 \end{aligned} \quad (8)$$

for fully developed turbulent flow  $C_\mu = 0.09$  and  $C_2 = 1.92$ ; for relaminarizing flows Jones and Launder [8] recommend,

$$\begin{aligned} C_\mu &= 0.09 \exp[-2.5(1.0 + R_T/50)] \\ C_2 &= 2.0 [1.0 - 0.3 \exp(-R_T^2)] \\ R_T &= \frac{\rho k^2}{\epsilon} \end{aligned} \quad (9)$$

However, these expressions have not given successful predictions of flows undergoing forward transition (e.g., [11]). An alternate transition model was developed by Shamroth and Gibeling [10] and was successfully applied to the time-dependent airfoil flow field problem. This method used the turbulence kinetic energy equation excluding the low Reynolds number correction term (last term in Eq. (1)), in conjunction with an algebraic length scale relation.

The analysis of [10] follows the integral turbulence energy procedure of [12-14] by introducing a turbulence function  $a_1$ ,

$$a_1 = C_\mu^{1/2} / 2 \quad (10)$$

and  $a_1$  is taken as a function of a turbulence Reynolds number,  $R_\tau$ , of the form

$$a_1 = a_0 \left[ \frac{f(R_\tau)}{100} \right] / \left\{ 1.0 + 6.66 a_0 \left[ \frac{f(R_\tau)}{100} - 1 \right] \right\} \quad (11)$$

where

$$\begin{aligned} a_0 &= .0115 \\ f(R_\tau) &= 100 R_\tau^{0.22} \quad R_\tau \leq 1 \\ f(R_\tau) &= 68.1 R_\tau + 614.3 \quad R_\tau \geq 40 \end{aligned} \quad (12)$$

and a cubic curve fit was used for values of  $R_\tau$  between 1 and 40. Since [12-14] used an integral procedure an average value of  $R_\tau$  was defined. In [10], a local value of  $R_\tau$  was defined as

$$R_\tau = \frac{\mu_\tau}{\mu} \quad (13)$$

Then  $a_1$  was evaluated via Eq. (11) and  $C_\mu$  follows from Eq. (10). The transition model of [10] was utilized in several of the cases presented herein; each with an appropriately specified algebraic length scale relation.

#### Turbulence Length Scale

An algebraic length scale relation is required in the turbulence model utilizing only the turbulence kinetic energy equation. The near wall region mixing length is obtained from the McDonald-Camarata model [15] with Van Driest damping [16],

$$l = l_\omega \tanh \left[ \frac{\kappa y}{l_\omega} \right] \left[ 1 - \exp(-y^+/A^+) \right] \quad (14)$$

where  $\kappa$  is the von Karman constant and  $A^+$  is the van Driest damping coefficient,

$$\kappa = 0.4 \quad (15)$$

$$A^+ = 26.0$$

and  $l_\omega = .09\delta$ , with the boundary layer thickness  $\delta$  to be specified.

The nondimensional distance  $y^+$  is defined as

$$y^+ = y \left( \frac{\rho U_\tau}{\mu} \right) \quad (16)$$

and the friction velocity  $U_\tau$  in the present analysis is taken as

$$U_\tau = \left( \frac{\tau_\ell}{\rho} \right)^{1/2} \quad (17)$$

where the local shear stress  $\tau_\ell$  is obtained from

$$\tau_\ell = \mu_{\text{eff}} (2 \bar{\mathbf{D}} : \bar{\mathbf{D}})^{1/2} \quad (18)$$

Note that for small  $y$  the tanh function in Eq. (14) reduces to  $ky$  while for large  $y$  it approaches  $l_\infty$ .

A more detailed description of the actual turbulence models used for the computation and their effect on the computation is given in the results section.



## RESULTS

As part of the present effort, several test cases were computed from the 1980-81 AFOSR-HTTM-Stanford Conference on Complex Turbulent Flows. Case number 0423, the primary case computed under this effort, considers the incompressible flow over a backward-facing step with a  $10^\circ$  turning downstream of the step. This was a predictive case for which the experimental results were not provided until after the conference. Case numbers 8601 and 8641 were funded primarily by the U.S. Army Research Office with computer resources funded by AFOSR. Case 8601 considers the compressible flow in a tube containing a normal shock wave. The data for this case was taken by Mateer, Brosh and Viegas [17]. Case 8641 considers a planar free-shear layer generated by a backward facing step, reattacking on a  $20^\circ$  ramp at supersonic speed. The data for this case was taken by Settles, Baca, Williams and Bogdonoff [18].

### Stanford Case 0423

A schematic of the geometry for this case is presented in Fig. 1. A coordinate system (Fig. 2) for this geometry was developed under the present effort beginning with Cartesian coordinates upstream of the step, followed by a transition region in which straight transverse coordinate lines ( $y^2$ -direction) are rotated through 10 degrees, and ending with another Cartesian region at the final 10-degree angle.

Two turbulence models were investigated using this test case. First, the two-equation ( $k$ - $\epsilon$ ) model with the Jones-Launder  $C_\mu(\mu_t)$  relationship was utilized. Preliminary computations were carried out for the channel upstream of the step in Fig. 1, in order both to verify the  $k$ - $\epsilon$  formulation in the computer code and to obtain consistent upstream flow conditions for the backstep problem. In the straight channel flow application the  $k$ - $\epsilon$  model, Eqs. (1-6, 8-9) gave quantitatively accurate predictions for boundary layer velocity profiles, skin friction, and flow development. However, when the model was applied to the backstep configuration numerical difficulties in solving the equations were encountered and converged solutions could not be obtained. These problems were found to be directly related to the low turbulence Reynolds number correction terms in Eq. (1,3). These terms are ad hoc differential terms which were devised by [8] for an attached relaminarizing boundary layer. In the separated shear layer which occurs downstream of the step the shearing terms (i.e.  $2\bar{D}:\bar{D}$ ) increase substantially

with a concurrent increase in both  $k$  and  $\epsilon$  in that region. The large gradients in  $k$ ,  $\epsilon$  and the velocities lead to large low Reynolds number correction terms. This results in nonphysical behavior such as excessively large turbulent viscosities in certain areas of the flow, and negative  $k$  and  $\epsilon$  in some areas. Numerous changes in the numerical treatment of these terms gave little improvement in the predictions, and several ad hoc modifications to the low Reynolds number correction terms did not improve the results.

Therefore, the  $k$ - $\epsilon$  model was abandoned for this case, and a turbulence kinetic energy model with an algebraic length scale relation, Eqs. (1,4-6,7-8, 10-18), was implemented. The mixing length distribution was constructed by using Eqs. (14-18) with the known boundary layer thicknesses upstream of the step, and an estimated thickness beyond the flow reattachment point on the lower wall in Fig. 1. In the region just downstream of the step, the length scale was varied smoothly from its upstream value to its downstream value. The computed flow field for this case exhibited a cyclic behavior in time and an absolute convergence to a steady solution could not be obtained. It is not known if this is physical behavior, or if it is caused by the turbulence model or the computational grid employed. Furthermore, the predicted reattachment point was about seventeen step heights downstream of the step which is considerably more than the experimentally observed value of 9.4 step heights [19]. A velocity vector plot for the predicted flow is shown in Fig. 3 at the last time step in the calculation. These results show an apparent anomalous behavior in the separated region, where the flow appears to be reattaching but then the separation region enlarges and continues much further downstream before actually reattaching. The reasons for this behavior are still under investigation; however, it may be related to the computational grid variation in that region if it is a nonphysical phenomena.

#### Stanford Case 8601

Case 8601 [17], which considers the compressible flow in a tube containing a shock wave, was computed by Roscoe and McDonald [20]. Although the geometry for this case is simple, the fluid mechanics is complicated because the stationary shock position in the tube is determined only by the boundary layer growth and the shock wave-boundary layer interaction. Thus, the physics of the near-wall turbulence phenomena must be modeled sufficiently well to

obtain meaningful results. This calculation was initiated with the  $\kappa$ - $l$  turbulence model described above with zero  $\kappa$  imposed as the wall boundary condition. The length scale specification is straightforward as long as the boundary layer remains attached in the interaction region. After the predicted flow field was well established in the  $\kappa$ - $l$  model calculation, the  $\kappa$ - $\epsilon$  model described above was introduced and the calculation was run to convergence. The boundary conditions for  $\kappa$  and  $\epsilon$  were both zero function values at the solid wall. Other boundary conditions used in the calculation are detailed in [20]. Also, a time-dependent adaptive mesh in the axial direction was implemented by [20] in order to properly resolve the shock at all times during the computation. The final computational mesh for this case is shown in Fig. 4 with the mesh lines near the tube wall omitted for clarity. There were a total of 41 mesh points in the radial direction with a high concentration near the wall for turbulent boundary layer resolution, and 31 mesh points in the axial direction with a concentration centered around the shock location.

Pressure contours in the vicinity of the shock are shown in Fig. 5. As expected, the shock is sharp in the core region and diffuses as the wall is approached due to the boundary layer interaction. In Fig. 6 the predicted wall pressure distribution is compared with the experimental results, and the agreement is seen to be quite good. A velocity vector plot from a radial location of  $0.5R$  to the tube wall is shown in Fig. 7. This figure clearly displays the shock-boundary layer interaction which results in boundary layer thickening and deflection of the outer flow, followed by recovery of the boundary layer downstream of the interaction region. The measured and predicted velocity profiles are compared in Fig. 8, where the agreement is quite good. The largest difference occurs at a streamwise location  $z/\delta_u = 8$ , which is in the recovery region fairly far downstream of the interaction region. Finally, the Reynolds stress profiles are compared in Fig. 9, where larger discrepancies between the experiment and predictions are observed. However, it is noted that data exhibits nonphysical behavior near the interaction region, probably due to probe interference or measurement difficulties in the transonic flow regime with a hot wire probe. Physically one expects the Reynolds stress to peak in the shear layer, and the location of that peak is not expected to shift nearly as much as indicated by the data. Although the two-equation turbulence model employed gives good mean flow predictions for this case, the

apparent problems with the Reynolds stress measurements do not permit any further evaluation of the model to be made.

#### Stanford Case 8641

Case 8641 [18] considers a planar free-shear layer generated by a backward facing step with reattachment on a  $20^\circ$  ramp at supersonic speed. The predictions presented here are taken from Weinberg, et al [21]. Settles, et al [18] carefully adjusted the experiment so that the free shear layer left the back step parallel to the wall without the expansion waves and subsequent recompression shock which would occur for a simple back step flow. As a result, the geometry (Fig. 10) which must be considered is more complicated. The computational domain developed by [21] for this case is shown in Fig. 11. The corner at the step was kept sharp since it has a significant influence on the flow field development, while the corner at the cavity-ramp juncture was rounded, since it was not expected to influence the reattachment appreciably.

The flow conditions for this case are  $M_\infty = 2.92$ ,  $Re_x = 6.7 \times 10^7$ /meter, and  $T_w = 265$  K. The boundary conditions for this problem are discussed by [21]. The turbulence model used was an algebraic mixing length model with the free stream length scale  $l_\infty$  linearly increased in the wake region downstream of the step until it reached a value of  $l_\infty = 0.09\delta_{avg}$ , where  $\delta_{avg}$  is the average boundary layer thickness on the ramp. This resulted in a value  $l_\infty = 0.039$  for the present case.

Predicted pressure contours are shown in Fig. 12. The compression waves generated by the reattachment coalesce into a shock as expected. The calculated velocity vectors presented in Fig. 13 show the shear layer parallel to the cavity wall, the presence of three vortices in the cavity, and the reattachment shock. Velocity profiles in the shear layer and on the ramp are compared with experimental data in Figs. 14 and 15. The agreement between the calculations and experiment is fairly good. The discrepancies which are observed are due in part to the mixing length turbulence model employed, the close proximity of the computation exit plane to the interaction region, and the lack of mesh refinement near the ramp wall [21].

### Turbulent Film Cooling Flow

Under the present effort a comparison with the turbulent film cooling experiment of Kadotani and Goldstein [2] has been initiated. Initially a mixing length turbulence model will be utilized. As part of the follow-on effort this case will be considered in more detail using both a turbulence kinetic energy-specified length scale model ( $k-l$ ), and a two-equation model ( $k-\epsilon$ ). The objective of this study is determination of an adequate turbulence model to permit accurate calculation of the film cooling flow field and a better understanding of the factors affecting the film cooling process.

## REFERENCES

1. Colladay, R.S. and Russell, L.M.: Streakline Flow Visualization of Discrete-Hole Film Cooling With Normal, Slant, and Compound Angle Injection, NASA TN D-8248, September, 1976.
2. Kadotani, K. and Goldstein, R.J.: Effect of Mainstream Variables on Jets Issuing from a Row of Inclined Round Holes, Journal of Engineering for Power, Vol. 101, 1979, p. 298.
3. Kreskovsky, J.P., Briley, W.R. and McDonald, H.: Computation of Discrete Hole Film Cooling Flow Using the Navier-Stokes Equations. Annual Technical Report, Contract F49620-78-C-0038, SRA Report R80-910002-2, May 1980.
4. Gibeling, H.J., Kreskovsky, J.P., Briley, W.R. and McDonald, H.: Computation of Discrete Hole Film Cooling Flow Using the Navier-Stokes Equations, Annual Technical Report, Contract F49620-78-C-0038, SRA Report R81-910002-3, June 1981.
5. Bergeles, G., Gosman, A.D. and Launder, B.E.: The Prediction of Three-Dimensional Discrete-Hole Cooling Processes: I-Laminar Flow, ASME Paper 75-WA/Ht-109, 1975.
6. Pratap, V.S. and Spalding, D.B.: Fluid Flow and Heat Transfer in Three-Dimensional Duct Flows, Int. J. Heat and Mass Transfer, Vol. 19, 1976, p. 1183.
7. Launder, B.E. and Spalding D.B.: The Numerical Computation of Turbulent Flows. Computer Methods in Applied Mechanics and Engineering, Vol. 3, 1974, pp. 269-289.
8. Jones, W.P. and Launder, B.E.: The Prediction of Laminarization with a Two-Equation Model of Turbulence. Int. J. Heat Mass Transfer, Vol. 15, 1972, p. 301.
9. Gibeling, H.J., Buggeln, R.C. and McDonald, H.: Development of a Two-Dimensional Implicit Interior Ballistics Code, U.S. Army Armament Research and Development Command, Ballistic Research Laboratory Report ARBRL-CR-00411, January 1980.
10. Shamroth, S.J. and Gibeling, H.J.: A Compressible Solution of the Navier-Stokes Equations for Turbulent Flow About an Airfoil, NASA CR-3183, 1979.
11. Quemard, C., and Michel, R.: Definition and Application of Means For Predicting Shear Turbulent Flows in Turbomachines. ASME Paper 76-GT-67, 1976.
12. McDonald, H. and Fish, R.W.: Practical Calculation of Transitional Boundary Layers, Int. J. Heat and Mass Transfer, Vol. 16, No. 9, 1973, pp. 1729-1744.

13. Shamroth, S.J. and McDonald, H.: Assessment of a Transitional Boundary Layer Theory at Low Hypersonic Mach Numbers. Int. J. Heat and Mass Transfer, Vol. 18, 1975, pp. 1277-1284.
14. Kreskovsky, J.P., Shamroth, S.J. and McDonald, H.: Application of a General Boundary Layer Analysis to Turbulent Boundary Layers Subjected to Strong Favorable Pressure Gradients. J. Fluid Eng., Vol. 97, June 1975, pp. 217-224.
15. McDonald, H. and Camarata, F.J.: An Extended Mixing Length Approach for Computing the Turbulent Boundary Layer Development, Proceedings Computation of Turbulent Boundary Layers - 1968 AFOSR-IFP Stanford Conference, Vol. 1, pp. 83-98, 1969.
16. Van Driest, E.R.: On Turbulent Flow Near a Wall. Journal of the Aeronautical Sciences, November 1956.
17. Mateer, G.G., Brosh, A. and Viegas, J.P.: A Normal Shock-Wave Turbulent Boundary Layer Interaction at Transonic Speeds, AIAA Paper 76-161, Jan. 1976.
18. Settles, G.S., Baca, B.K., Williams, D.R. and Bogdonoff, S.M.: A Study of Reattachment of a Free Shear Layer in Compressible Turbulent Flow, AIAA Paper 80-1408, July 1980.
19. Eaton, J.K.: Summary of Computations for Cases 0421, 0431, P2, and P3; Separated Internal Flows, 1980-81 AFOSR/HTTM/Stanford Conference on Complex Turbulent Flows, Stanford University Department of Mechanical Engineering, Stanford, CA, 1982.
20. Roscoe, D.V. and McDonald, H.: Investigation of Transonic Shock-Wave/Boundary-Layer Interaction. (Report in preparation.)
21. Weinberg, B.C., McDonald, H. and Shamroth, S.J.: Navier-Stokes Computations of Aft End Flow Fields. Final Report, Contract DAAG29-79-C-0003, U.S. Army Research Office, May 1982.

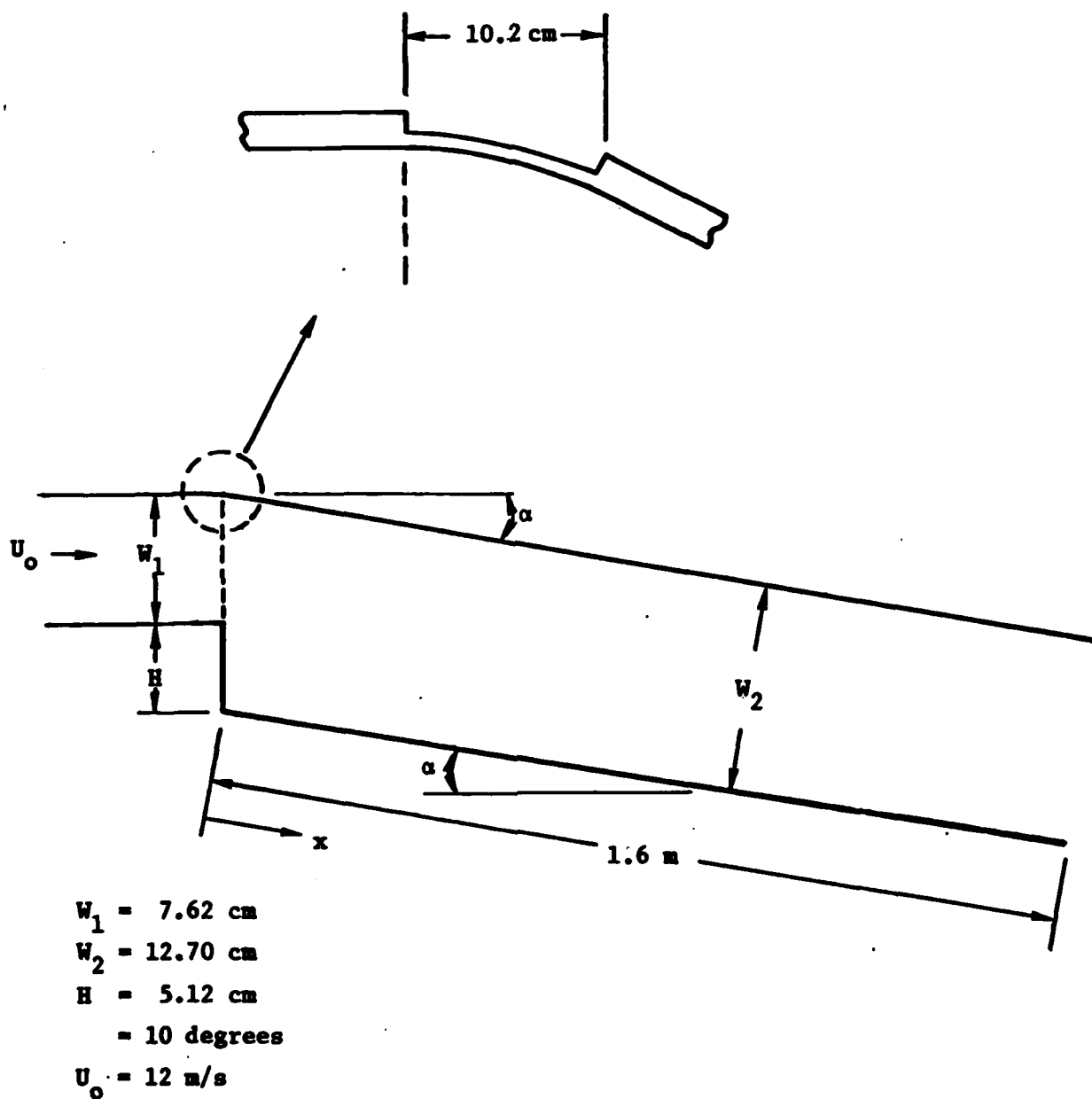


Figure 1 - Schematic of geometry for Stanford Case 0423.



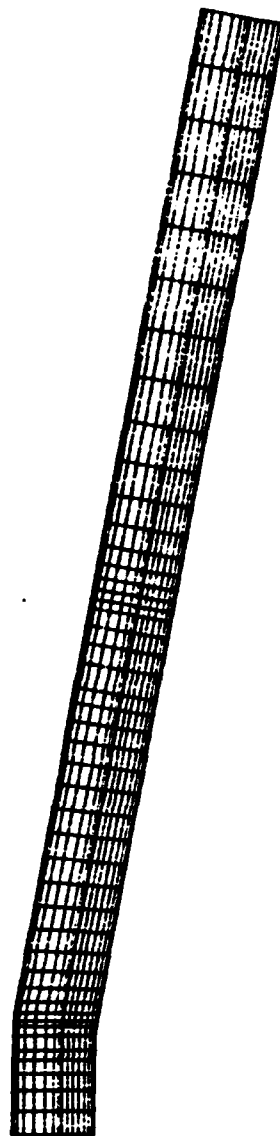


Figure 2 - Coordinate system for Stanford Case 0423 geometry.  
Certain coordinate lines omitted for clarity.

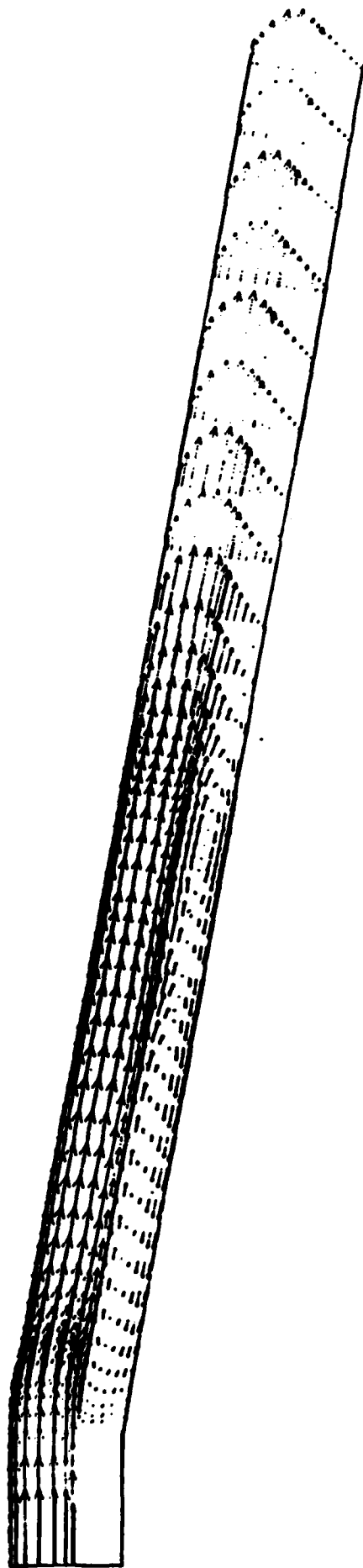


Figure 3 - Computed velocity vector plot, Stanford Case 0423

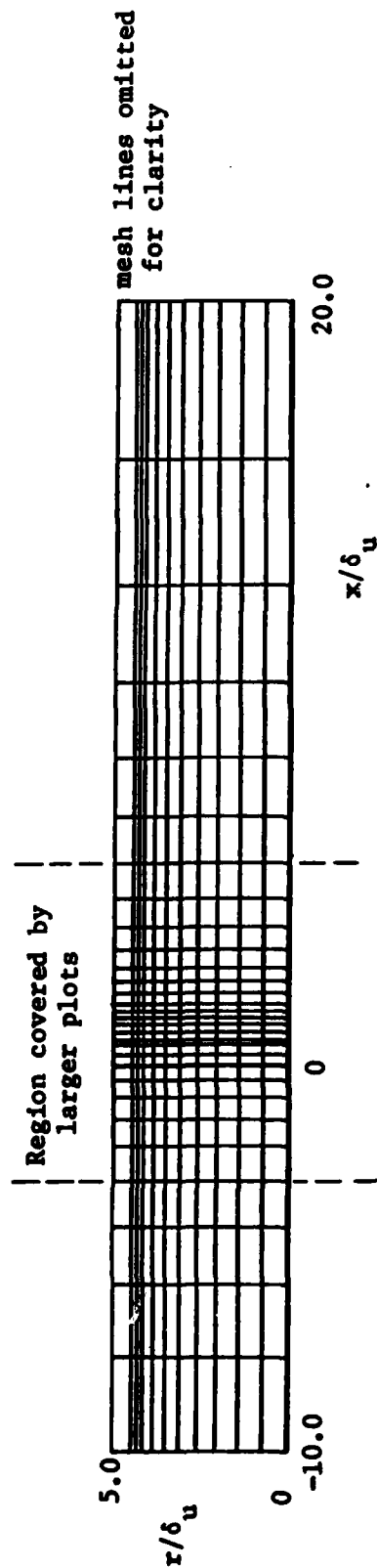


Figure 4 - Computational mesh for Stanford Case 8601: 41 radial lines by 31 axial lines.  $\delta_u$  is the upstream boundary layer thickness.

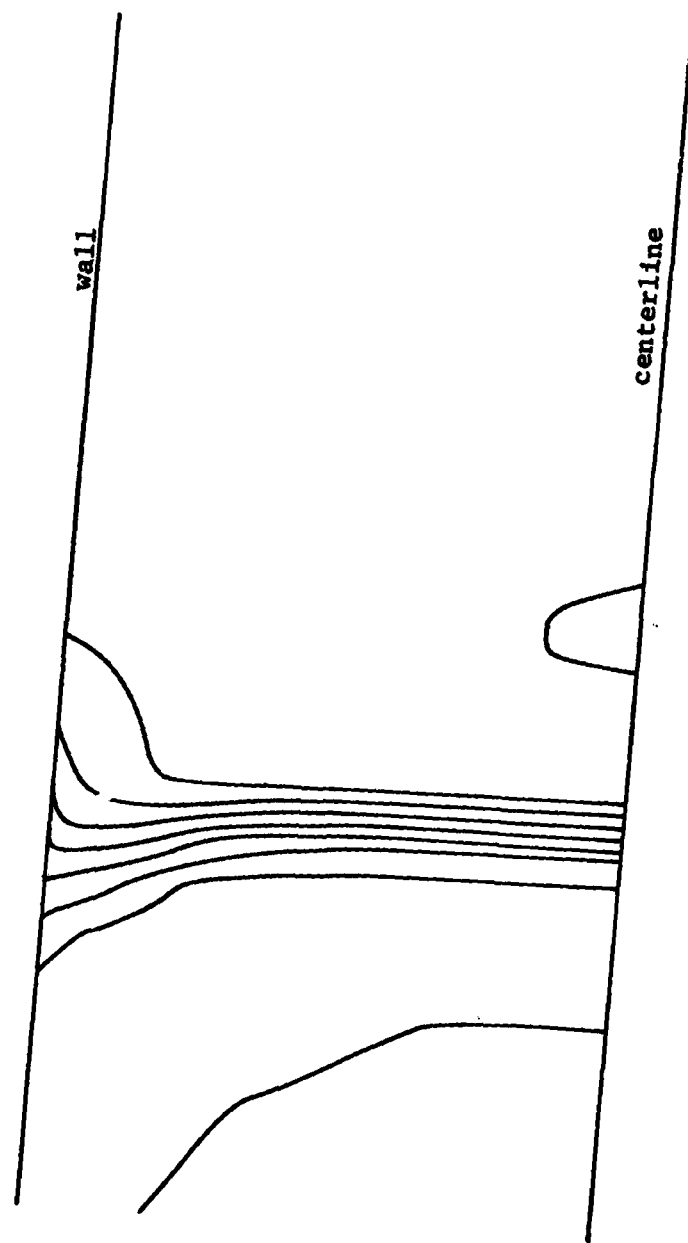


Figure 5 - Pressure contours in the vicinity of shock, Stanford Case 8601.

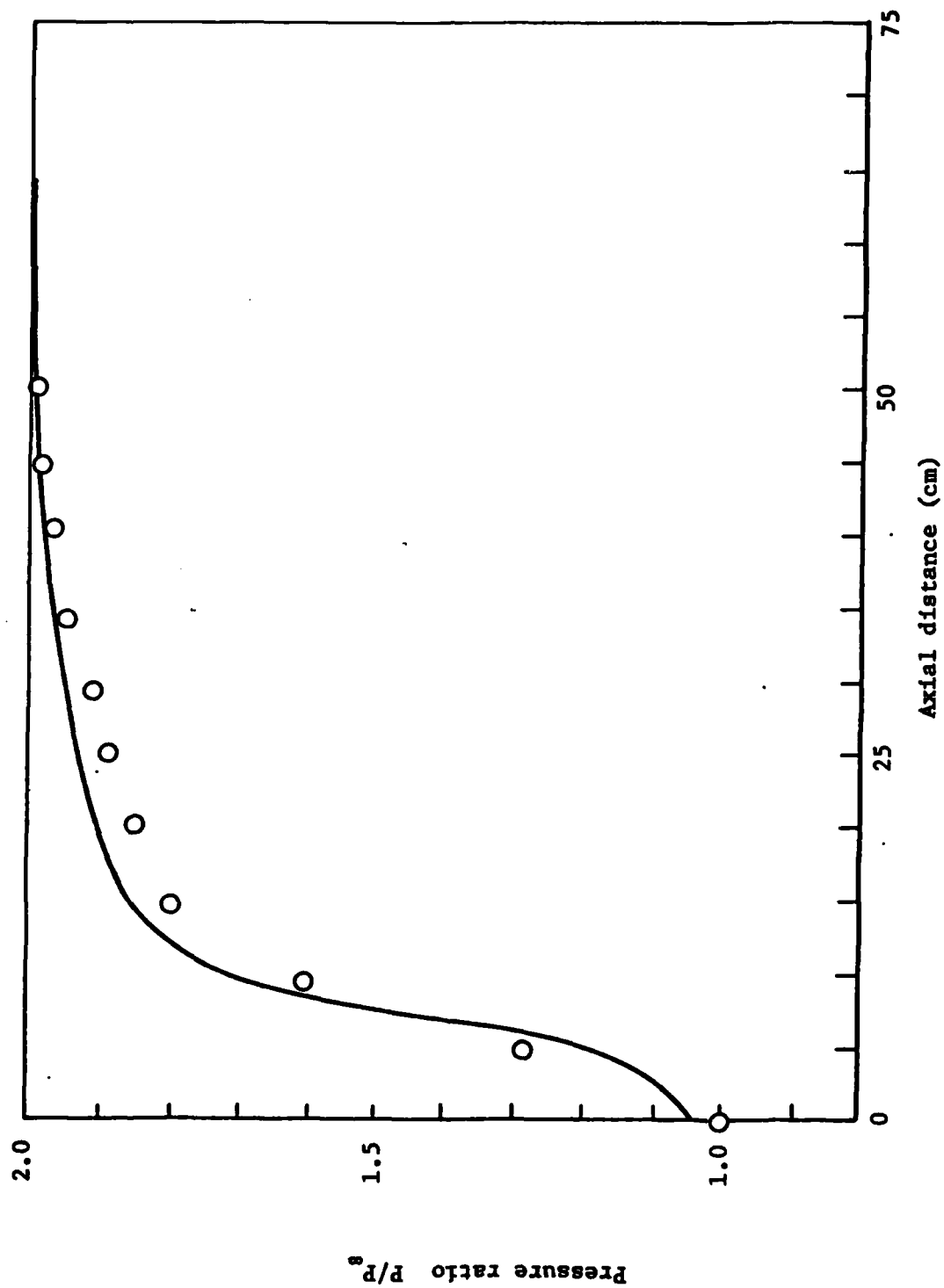


Figure 6 - Wall pressure distribution, Stanford Case 8601.

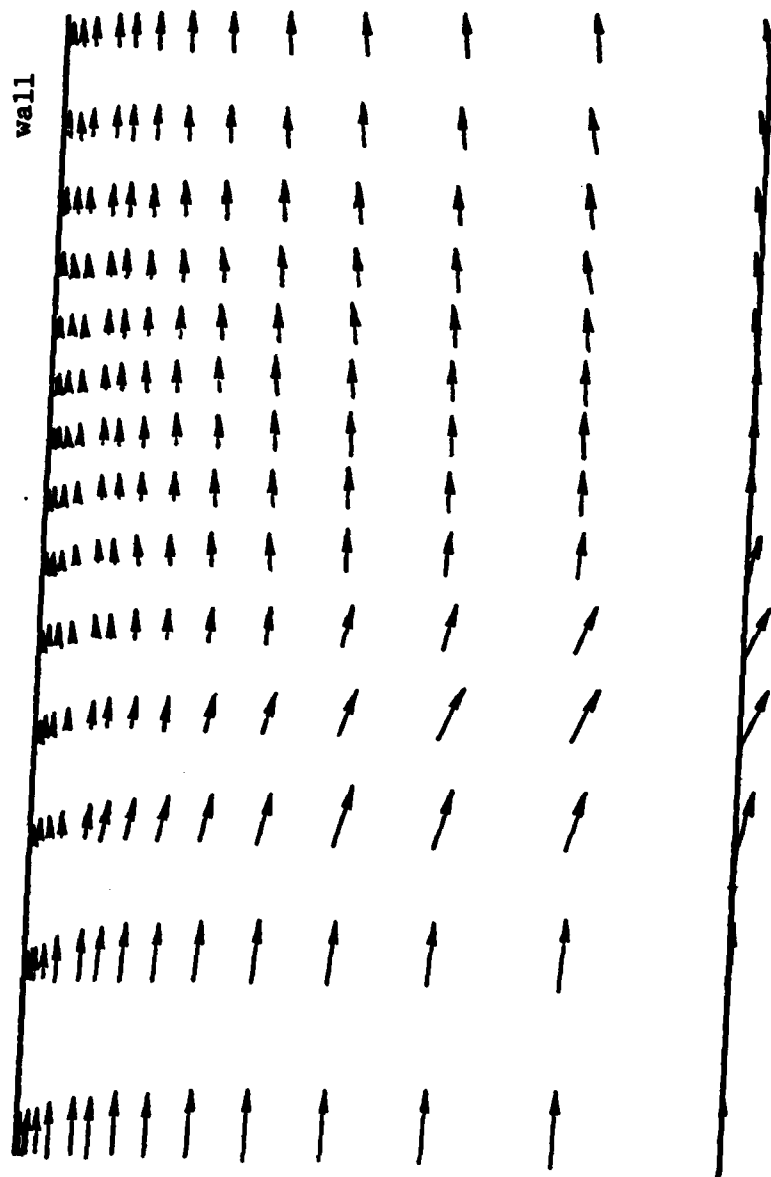


Figure 7 - Velocity vector plot near the wall showing shock boundary

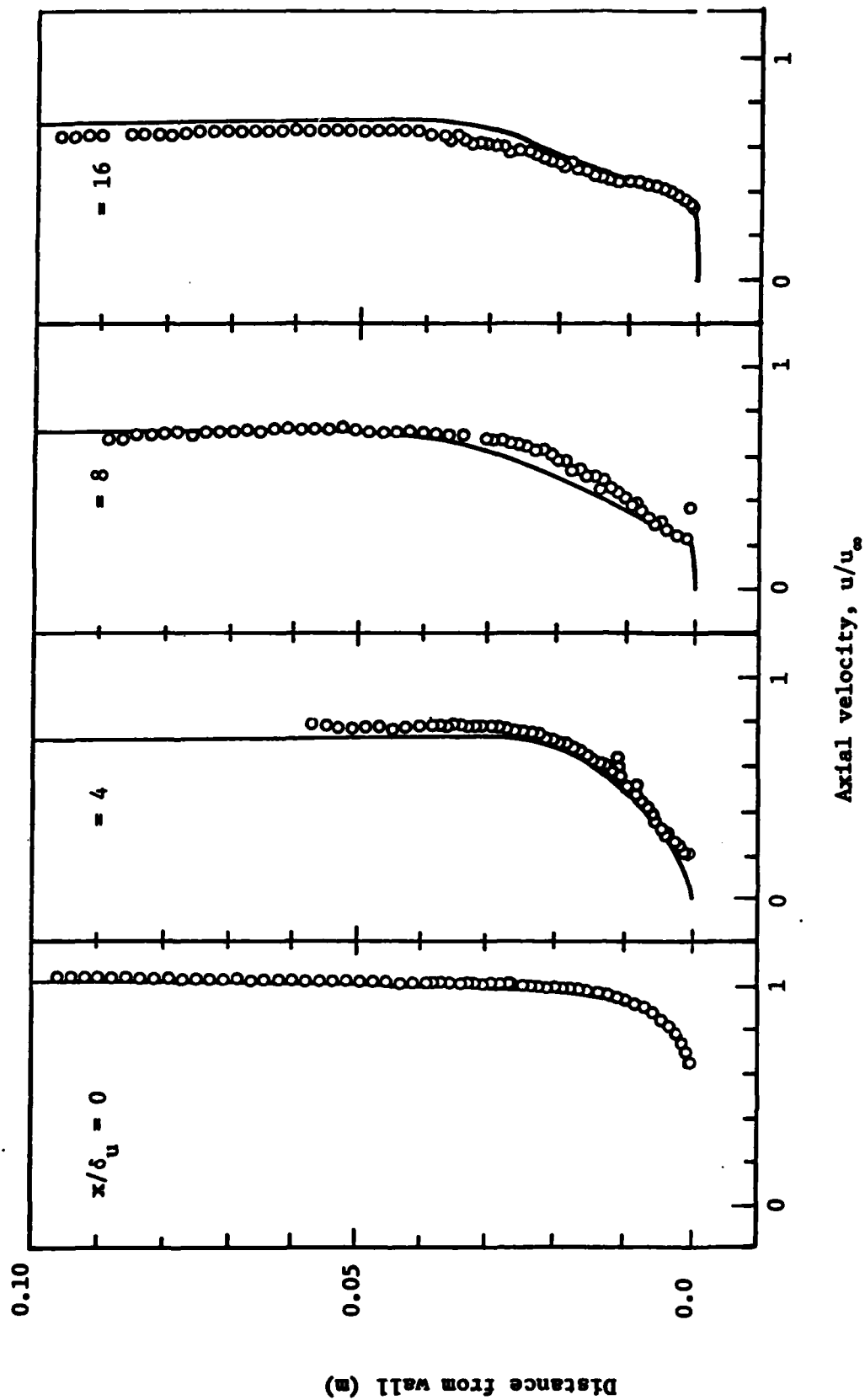


Figure 8 - Axial velocity profiles at selected axial locations, Stanford Case 8601.

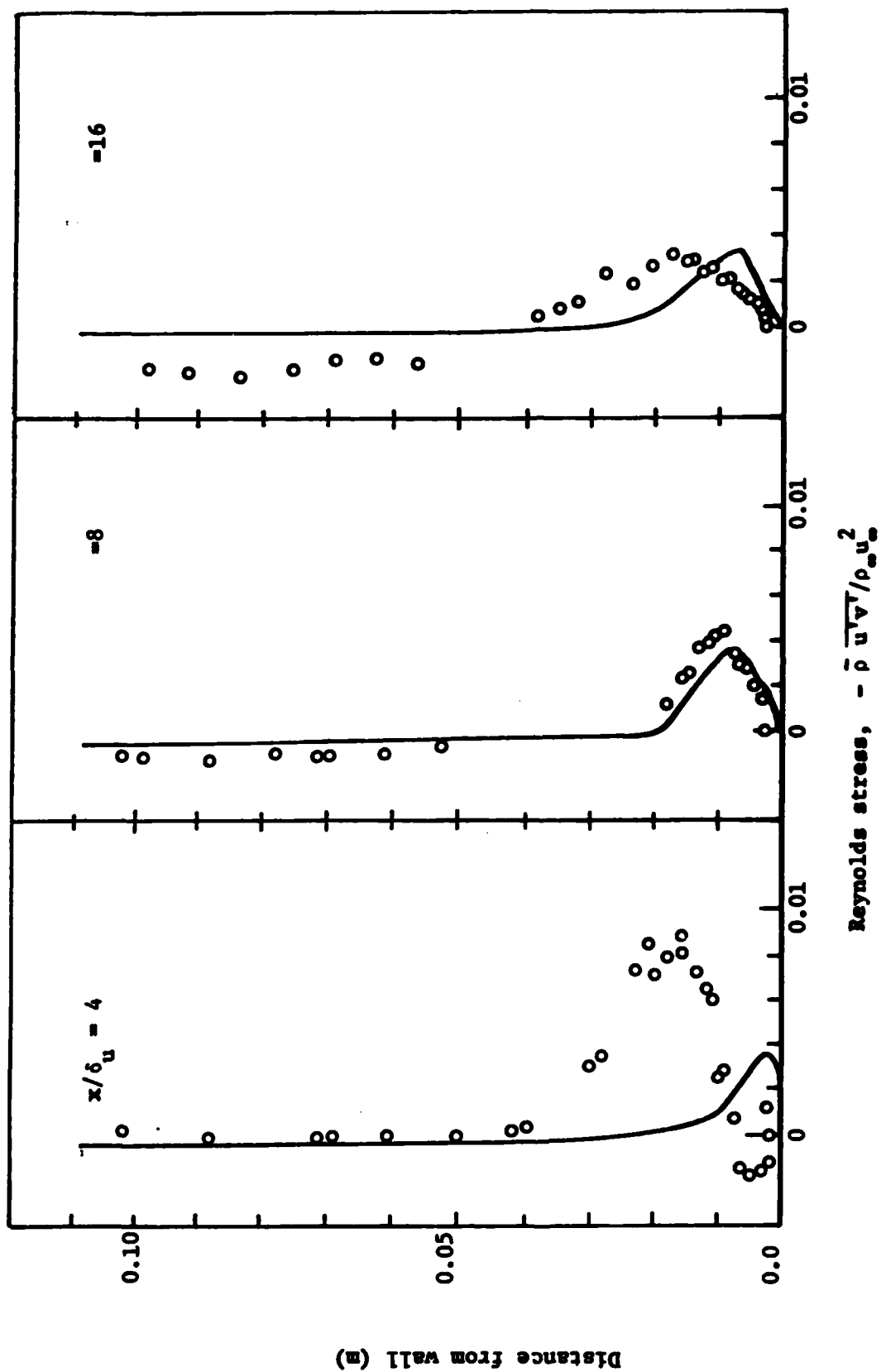
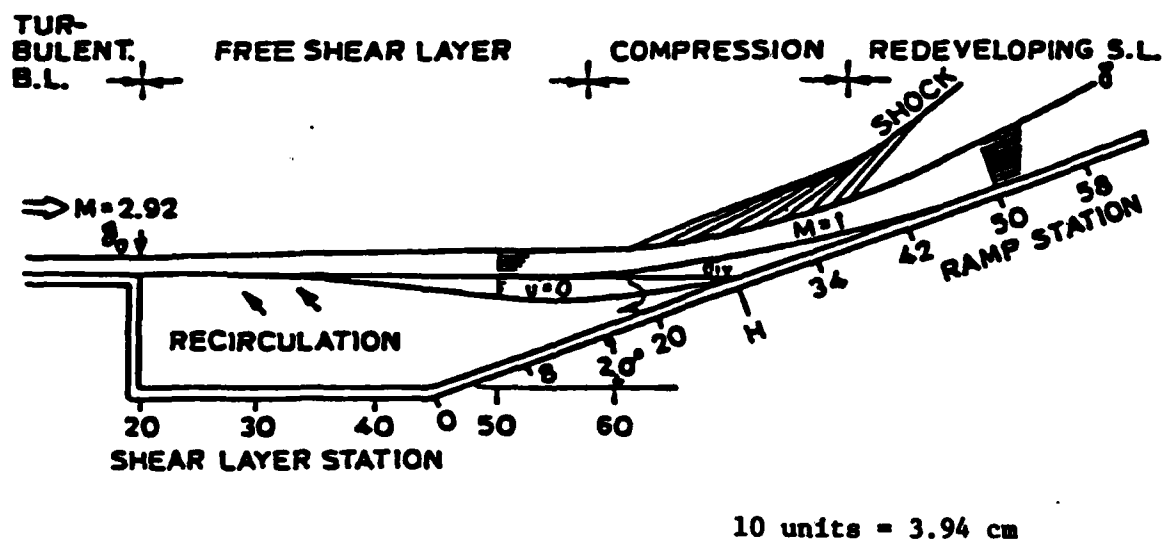


Figure 9 - Reynolds stress profiles at selected axial locations, Stanford Case 8601.



**CASE 8641 (SETTLES, BACA, WILLIAMS, BOGDONOFF, 1980)**



**Figure 10 - Schematic of Flow Field.**

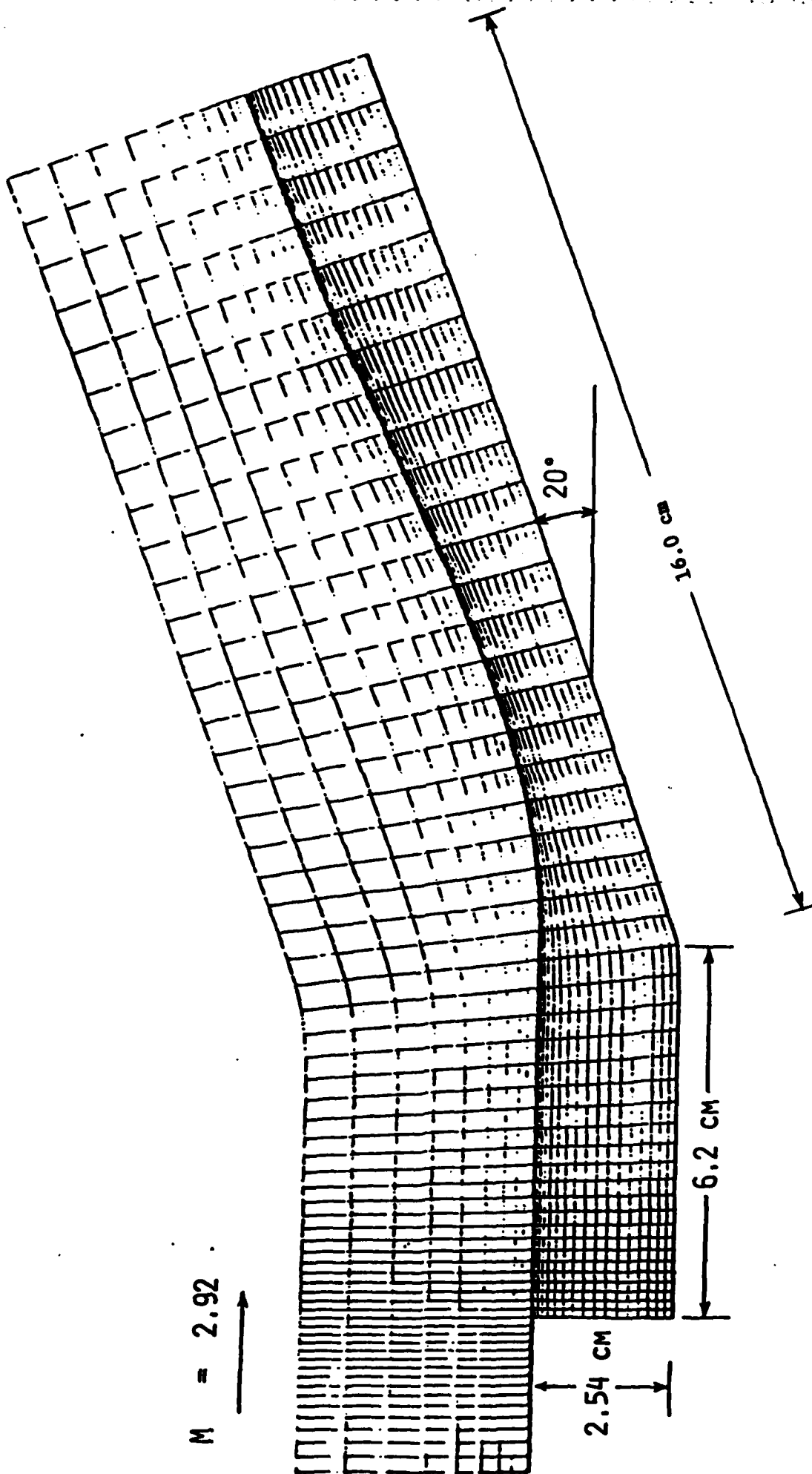


Figure 11 - Computational Domain.

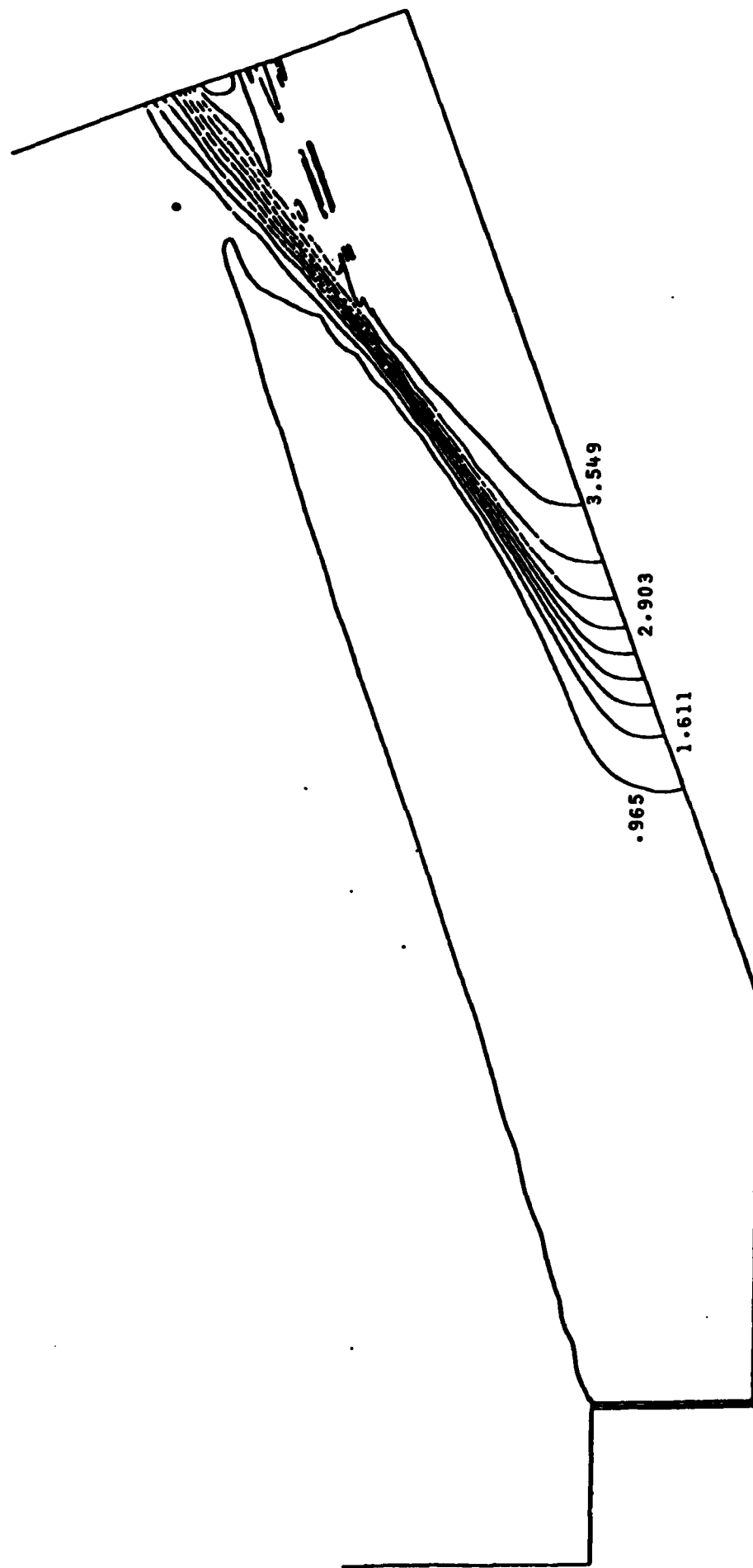


Figure 12 - Computed Contour Plot of Pressure.

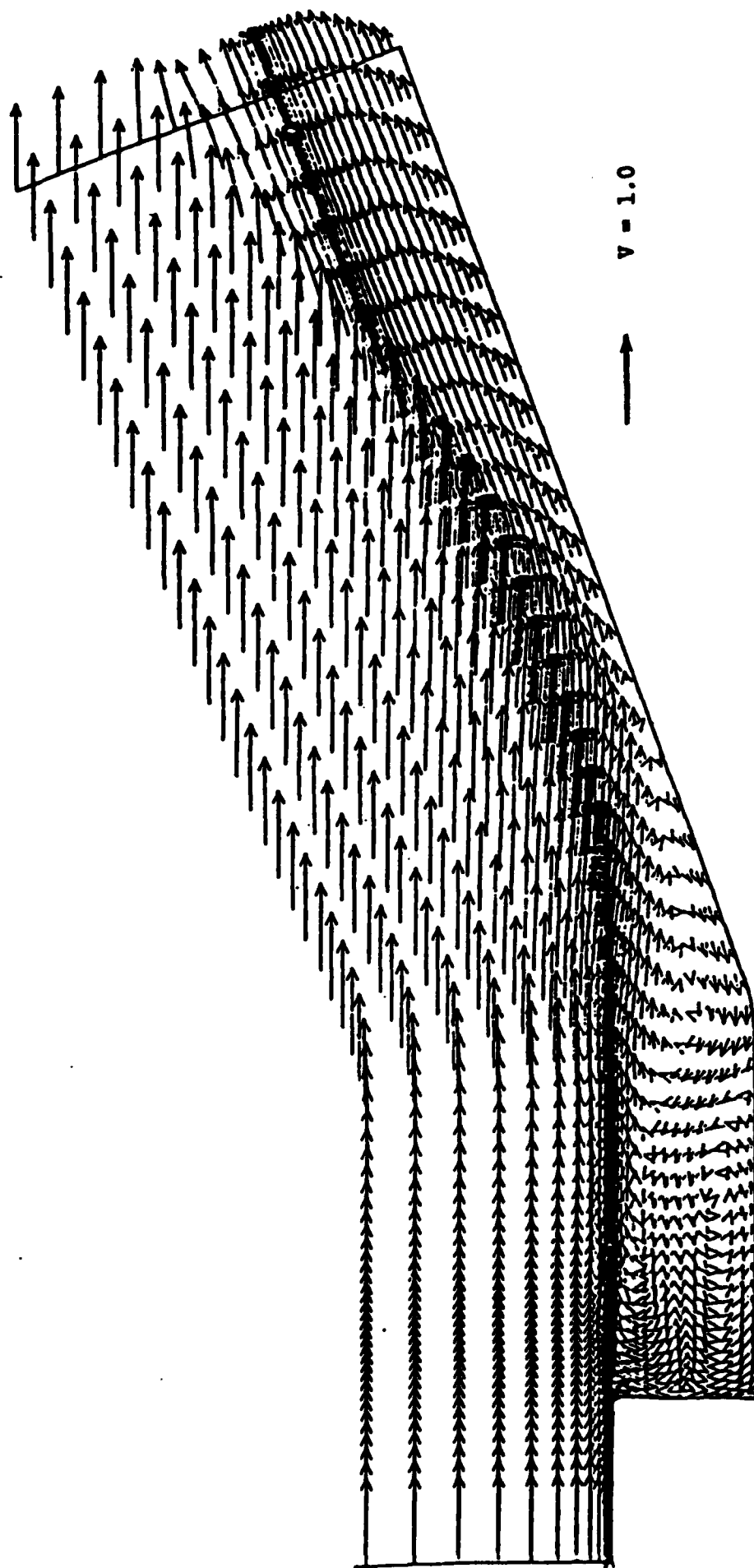


Figure 13 - Computed Velocity Vector Plot.

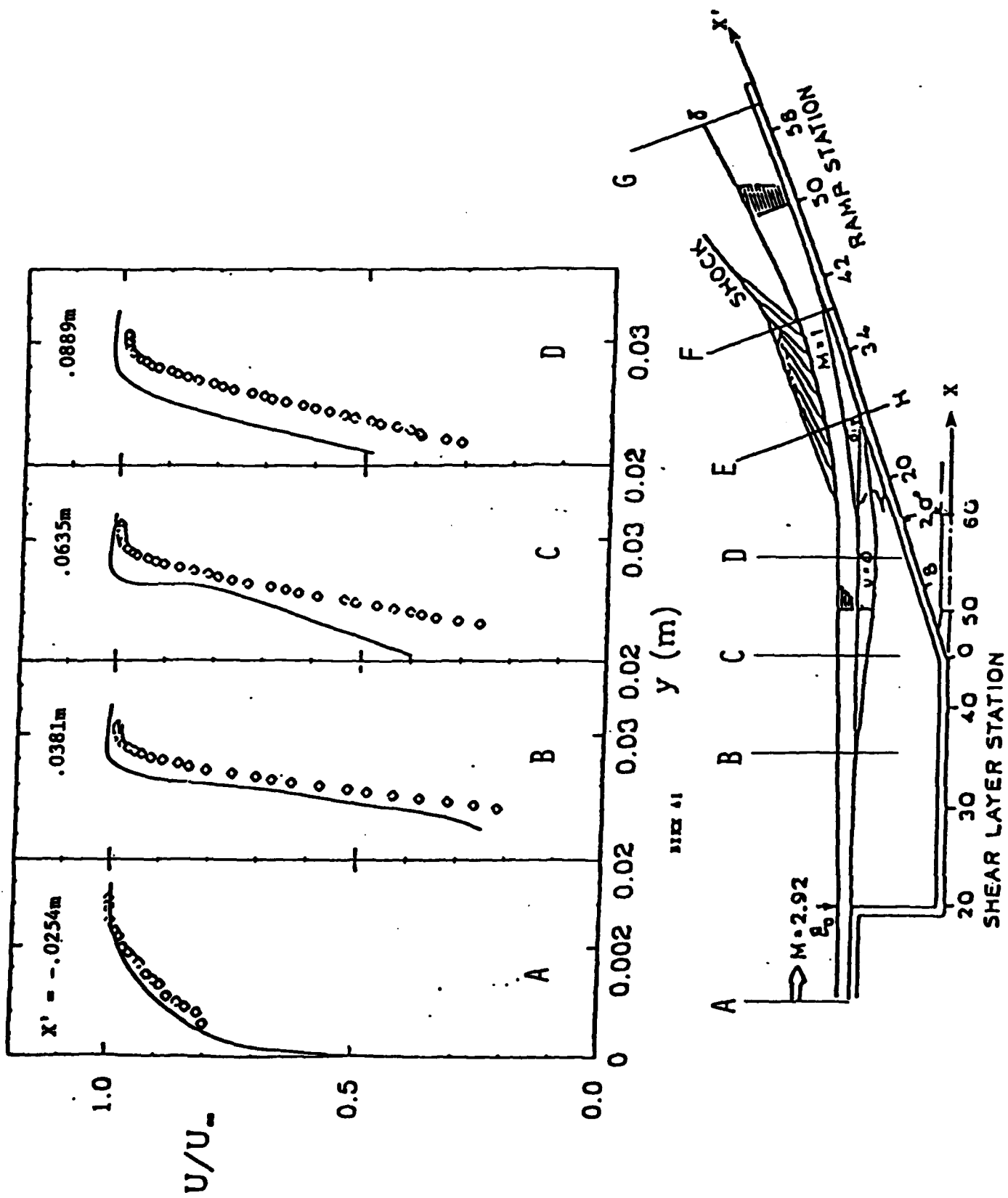


Figure 14 - Velocity Profiles Through Shear Layer.

